

Electronic crossover in the overdoped high-temperature (Y,Ca)Ba₂Cu₃O_y superconductor by Raman scattering

T. Masui,* T. Hiramachi, K. Nagasao, and S. Tajima

Department of Physics, Graduate School of Science, Osaka University, Machikaneyama 1-1, Toyonaka, Osaka 560-0043, Japan

(Received 13 August 2008; published 16 January 2009)

The electronic Raman scattering in overdoped (Y,Ca)Ba₂Cu₃O_y was investigated with changing hole concentration in the superconducting state. It was found that the superconducting responses such as the pair-breaking peaks in the A_{1g} and B_{1g} spectra and the anisotropy of the pair-breaking peak in XX and YY polarizations radically change at around the carrier doping $p=0.19$. Since both a - and c -axis resistivities strongly suggest the closing of pseudogap at $p\sim 0.18$, the observed change at $p=0.19$ in the superconducting Raman response is attributed to the electronic crossover due to the collapse of the pseudogap.

DOI: [10.1103/PhysRevB.79.014511](https://doi.org/10.1103/PhysRevB.79.014511)

PACS number(s): 74.25.Gz, 74.72.Bk

I. INTRODUCTION

A rough sketch of the electronic phase diagram for high- T_c superconducting cuprates (HTSCs) was established at the early stage of these 20 years of studies.¹ However, in spite of a tremendous amount of studies, we are still far from the complete understanding of the phase diagram. Compared to the underdoped electronic state governed by a mysterious pseudogap,² the overdoped state has been less studied so far. It is partly because the electronic state is supposed to merely approach a conventional Fermi-liquid metal.

Recently the overdoped state is re-examined in detail, in relation to a quantum critical point (QCP). Tallon and Loram³ insisted a QCP at the carrier doping level $p=0.19$ where the pseudogap energy estimated from specific heat falls to zero. A recent neutron experiment also suggested that the resonant magnetic modes show a qualitative change at the same doping level.⁴ On the other hand, there are reports that physical properties are clearly distinguished between the underdoped and overdoped regimes at the boundary of optimal doping $p=0.15-0.16$.⁵⁻⁷ The former results suggest that the pseudogap line and the T_c dome are independent in the phase diagram, which indicates that the pseudogap is irrelevant to the superconductivity pairing and not a precursor of superconductivity. By contrast, the latter facts support the picture in which the pseudogap is a precursor of superconductivity and thus its line merges to the T_c dome near the optimum doping, as is predicted by the t - J model^{8,9} and/or phase fluctuation model.¹⁰

One of the approaches to the phase diagram problem is to see the electronic change through the superconducting properties such as a superconducting gap. Among various experimental methods, Raman-scattering measurement has an advantage in determining the \mathbf{k} dependence of gap energy as a bulk property¹¹ in contrast to surface sensitive probes such as angle-resolved photoemission spectroscopy (ARPES). Thanks to this advantage, we have been studying superconducting gaps of YBa₂Cu₃O_y (Y123) by Raman-scattering technique. In the heavily overdoped sample Y_{0.88}Ca_{0.12}Ba₂Cu₃O_y, we found some anomalies in the pair-breaking peaks and interpreted them as the evidence of s -wave component admixture and an increase in chain-plane coupling.^{12,13} These phenomena are different not only from

the behaviors of optimally doped samples but also from those of the conventional Fermi-liquid-like metal (superconductor) expected in the overdoped regime. The next interest is how these anomalies develop with doping and how they link to the normal-state properties or the phase diagram.

To explore this issue, in the present study, we examined a precise doping dependence of Raman-scattering spectra between $p=0.16$ and 0.22 . We also measured a - and c -axis resistivities to monitor the normal state for the same series of crystals. When we discuss something related to the doping level in HTSC, it is very important to collect the data of various physical quantities for the same series of samples by fixing a material. Here we have chosen the Y123 system and prepared a series of detwinned crystals of Y_{1-x}Ca_xBa₂Cu₃O_y (Y/Ca123) with various x and y . Comparing the spectra for a certain doping level p but different y , we can distinguish the CuO-chain contribution from the response of the CuO₂ plane. It has been uncovered that the spectral changes are not monotonic with p but show an abrupt change near $p=0.19$ where the resistivity suggests the closing of pseudogap. The possibility for the CuO-chain contribution to the observed anomalies was completely ruled out.

II. EXPERIMENTS

Single crystals of Y/Ca123 were grown by a pulling technique¹⁴ for various Ca contents. Rectangular-shaped samples were cut from as-grown crystals and detwinned under uniaxial pressure, followed by postannealing in oxygen atmosphere to adjust oxygen content. Carrier doping level (p) was controlled by both Ca content (x) and oxygen content (y). Ca content was determined by an inductively coupled plasma analysis, while oxygen content was estimated from annealing temperature using the literature data¹⁵ given for each Ca content. 15 samples with different combination of x and y were prepared for Raman measurement and 26 for resistivity measurement in total. The value of x varies from 0 to 0.12, while y is from 6.74 to 6.92. The carrier concentration p was estimated from the empirical relation between T_c and p .¹⁶

Raman-scattering spectra were measured in the pseudo-backscattering configuration for various polarizations with using a triple monochromator equipped with a refrigerator

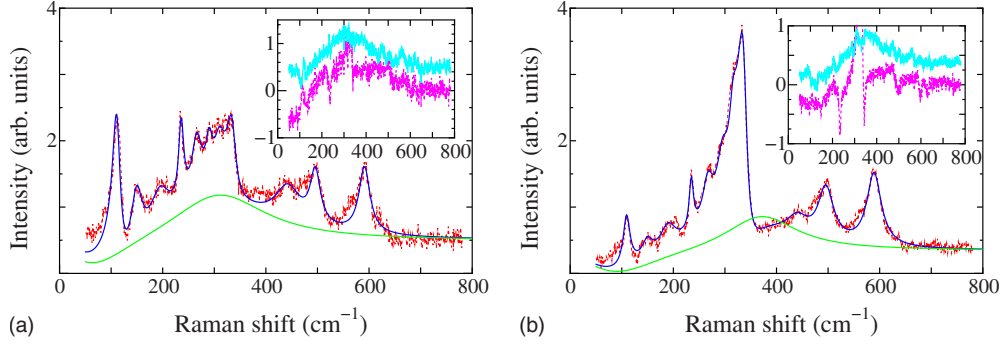


FIG. 1. (Color online) Raman-scattering spectra of $Y_{1-x}Ca_xBa_2Cu_3O_y$ for $x=0.10$, $y=6.83$, and $p=0.179$ with (a) A_{1g} and (b) B_{1g} polarizations. Solid (blue in color) curves are the fitting results by the Green's-function method and the light solid (green in color) is the extracted electronic responses. Insets show electronic response (solid line, cyan in color) and differences between the spectra at 10 and 100 K, $I(10\text{ K}) - I(100\text{ K})$ (dotted line, pink in color).

cryostat. Although the crystal structure of Y/Ca-123 is orthorhombic, all symmetries refer to a tetragonal D_{4h} point group in the present study. X and Y axes are indexed perpendicular to and along the Cu-O chains, while X' and Y' are rotated by 45° from X and Y , respectively. In order to extract the electronic Raman response, we fit the spectra in the same way as in Ref. 17.

Resistivity was measured by means of a standard four-probe technique. ρ_a was measured for detwinned samples, while crystals for ρ_c measurements were not detwinned. So far, there has been no available result of ρ_c for heavily overdoped Y/Ca123 because the measurements for c -axis properties are difficult with polycrystalline samples or thin single crystals grown by a flux method. It should be mentioned that Y123 single crystals grown by a pulling technique is as long as a few millimeters along the c axis, which enables us to measure ρ_c accurately.

III. RESULTS

A. Raman-scattering spectra with A_{1g} and B_{1g} symmetries

Figure 1 shows the Raman-scattering spectra of Y/Ca-123 for $x=0.103$ and $y=6.83$ with A_{1g} ($X'X' - XY$) and B_{1g} ($X'Y'$) polarizations at 10 K. Compared to the spectra of optimally doped Y123 ($x=0$ and $y=6.88$),¹⁸ there appear several sharp peaks ascribed to the phonons induced by oxygen deficiencies. The obtained A_{1g} and B_{1g} electronic Raman spectra (green curves) show broad peaks (pair-breaking peaks) centered at around 300 and 400 cm^{-1} , respectively, which are due to the modification of the electronic component below the superconducting transition temperature T_c . The inset of Fig. 1 compares the electronic component at 10 K and the difference of the raw spectra at 100 and 10 K. The good correspondence between the two curves justifies our fitting procedure.

Figure 2 shows gradual changes in the 10-K-electronic responses with carrier doping for the A_{1g} and B_{1g} polarizations. In the B_{1g} spectra the pair-breaking peak shifts more rapidly to lower energies than in the A_{1g} spectra. This decrease is, as expected from the suppression of T_c , partly due to the decrease in the superconducting gap energy itself but is too large to be explained with such a usual mechanism.

The difference between B_{1g} and A_{1g} pair-breaking peak energies becomes small with carrier doping. In the electronic Raman scattering of cuprates, the difference between the polarizations is explained by the screening effect, which is usually effective only for A_{1g} polarization.¹⁹ But in the present case, some mechanisms are necessary to suppress the peak energy in B_{1g} polarization. Another remarkable change appears in peak intensity. The intensity of the A_{1g} peak decreases with doping, while that of the B_{1g} peak increases. All these changes were reported in our previous paper¹² and were discussed as the effect of s -wave component mixing ($\sim 20\%$ at $p=0.22$) into a d -wave gap.²⁰

The B_{1g} and A_{1g} peak energies and the peak intensity ratio $I(A_{1g})/I(B_{1g})$ are plotted in Figs. 3(a) and 3(b). One can find a clear kink at $p \sim 0.19$ in the A_{1g} peak energy, while the B_{1g} peak energy rapidly decreases with doping and merges to the A_{1g} line at $p > 0.19$. Here we note that if we plot the same quantities as a function of oxygen deficiency $7-y$, no systematic change is observed, as demonstrated in the inset. This implies that the observed phenomena are caused only by carrier doping but related to neither the CuO-chain structure nor the oxygen deficiency in it. The peak intensity ratio also drops with doping and reaches about 0.5 at $p \sim 0.19$, above which it is almost constant. All these results suggest that there is a qualitative difference in the electronic state at $p < 0.19$ and $p > 0.19$.

B. Raman-scattering spectra with XX and YY polarizations

Another marked effect of carrier overdoping is the quantum interference between Raman scattering of CuO chains and CuO₂ planes.¹³ It manifests itself as a strong suppression of the pair-breaking peak in the YY -polarization spectrum. As is typically seen in the Fano line shape for the electron-phonon coupling system, the interference between two electronic Raman-scattering processes modifies a Raman spectrum if the coupling of these two electronic channels is strong. Therefore, the suppression of pair-breaking peak in the YY spectrum is an indication of a large transfer matrix between the CuO₂ plane and CuO chain in the heavily overdoped Y/Ca123.

A precise doping dependence of the electronic Raman

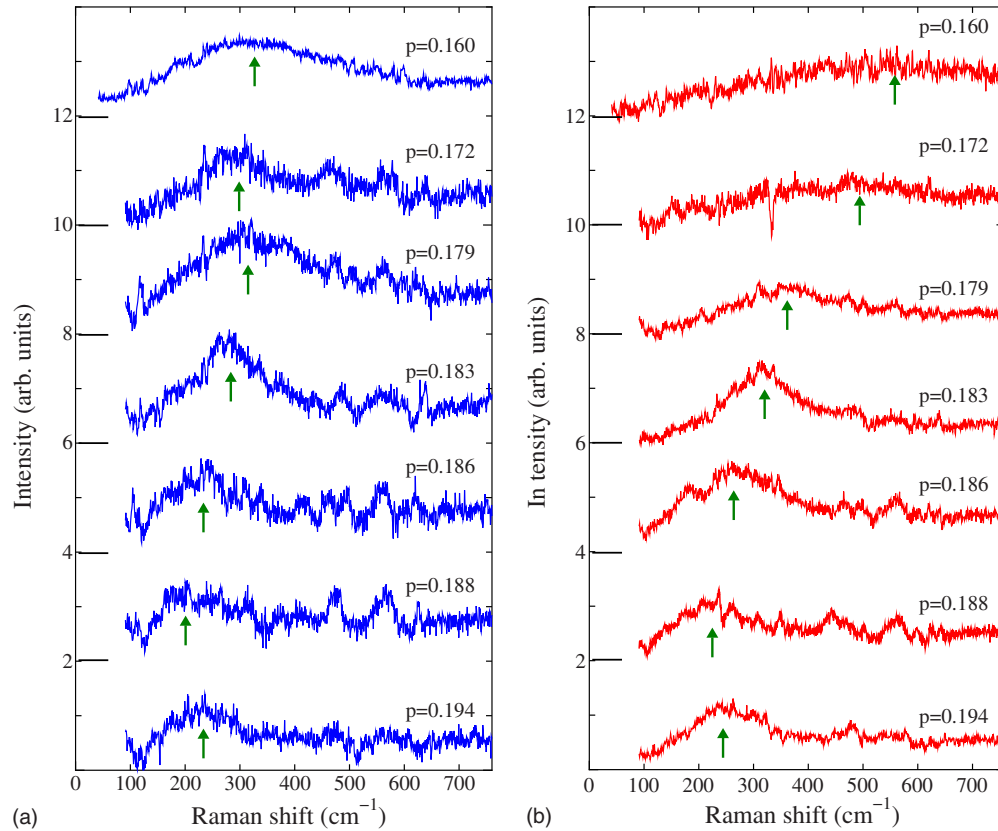


FIG. 2. (Color online) Doping dependence of the electronic responses in the (a) A_{1g} and (b) B_{1g} Raman scatterings ($T=10$ K). Phonon peaks are subtracted by fitting.

spectra of XX and YY polarizations is demonstrated in Fig. 4. It is seen that the suppression of the YY -polarization peak sets in at around $p=0.19$ and then grows with further doping. The suppression in the YY polarization is not caused by oxygen deficiency in the CuO chain but develops as a function

of doping level. Namely, this quantum interference effect is enhanced by the increase in hole concentration on CuO_2 planes. This is another support for the electronic change at $p \sim 0.19$. Here we note that the radical shift of B_{1g} peak in the tetragonal framework is not an artifact caused by the XY

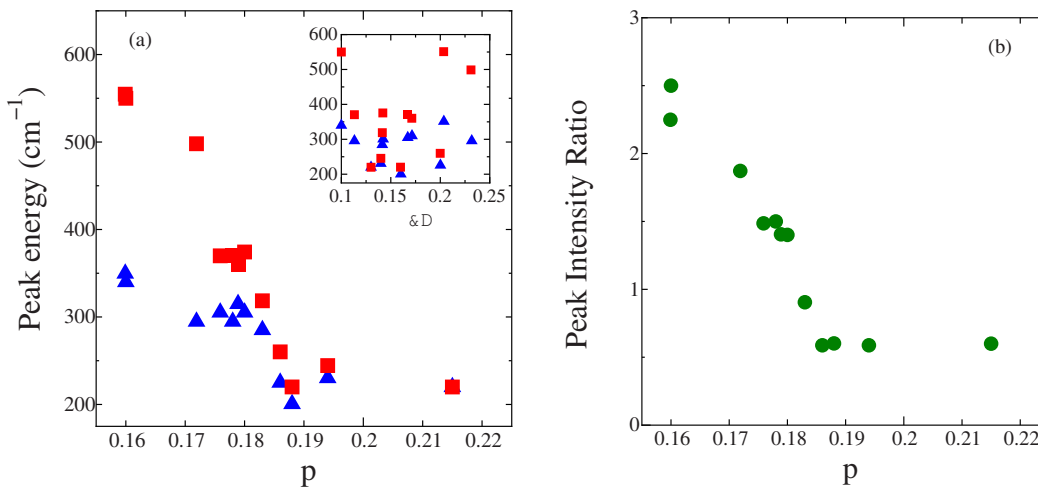


FIG. 3. (Color online) (a) Doping (p) dependence of the pair-breaking peak energies for A_{1g} and B_{1g} spectra. Inset shows the peak energies as a function of oxygen deficiency $\delta=7-y$. Squares and triangles are the data for B_{1g} and A_{1g} peaks, respectively. (b) Doping dependence of the peak intensity ratio $I(A_{1g})/I(B_{1g})$.

anisotropy. It is because the XY anisotropy becomes remarkable at $p > 0.19$, while the radical shift of B_{1g} peak is observed at $p < 0.19$. The presence of CuO chain is essential for the former phenomenon, but it plays no role in the latter.

C. Resistivity in the a and c directions

It is important that the doping level $p \sim 0.19$ is a common boundary for the two anomalies in the A_{1g}/B_{1g} spectra and the XX/YY spectra. This implies that some distinct change in the electronic state is behind them. To discuss the change at ~ 0.19 , the resistivity data are helpful and suggestive. Figure 5 shows the temperature dependence of resistivity along the a and c axes of Y/Ca123 crystals. Since it is a collection of the data for samples with various Ca contents, the doping level does not correlate with oxygen content. Both ρ_a and ρ_c monotonically decrease with doping. It is rather surprising that ρ_c is not much affected by oxygen deficiency. A signature of pseudogap opening can be seen in the upward deviation of $\rho_c(T)$ from the T -linear relation as well as the downward deviation of $\rho_a(T)$ from the T -linear relation.²¹ Figure 5 demonstrates that the pseudogap temperature T^* is lowered with doping and becomes invisible above $p \sim 0.18$. If we extrapolate the $T^*(p)$ line below T_c in the phase diagram, it is expected to reach zero at $p \sim 0.19$. This is consistent with the result of Tallon and Loram.³

IV. DISCUSSION

Since a strong two dimensionality beyond the band theory in HTSC is predominantly due to strong electron correlation but enhanced by the pseudogap opening, the close of pseudogap is expected to weaken two dimensionality by increasing interlayer coupling. On one hand, the close of pseudogap at $p \sim 0.19$ is strongly suggested by the disappearance of $T^*(p)$ in Fig. 5. On the other hand, the negative quantum interference seen in Fig. 4 is caused by an increase in the transfer matrix between CuO chain and CuO₂ plane, namely, three-dimensional coupling between the layers. Therefore, it is likely that the negative quantum interference starting at $p=0.19$ is caused by the close of the pseudogap. It can be considered as the evidence for recovering of three dimensionality above $p=0.19$.

Here it should be noted that even after the pseudogap disappears anisotropy in the normal state cannot be described by an effective-mass model. This can be seen, for example, in the temperature dependence of the resistivity ratio ρ_c/ρ_a which should be constant in a Fermi-liquid metal. The value of resistivity ratio (~ 6 at 90 K) is also much larger than the band calculation value. Therefore, judging from the normal state, we should say that the electronic state does not return to a three-dimensional state in the present doping range. This seems to be inconsistent with the above statement based on the Raman response in the superconducting state. However, it is not obvious whether anisotropy ratios estimated from the normal and superconducting state properties are the same or not. It is necessary to examine anisotropy in the superconducting state.

In the superconducting state, two dimensionality of HTSC is observed in an extremely short coherence length in the c

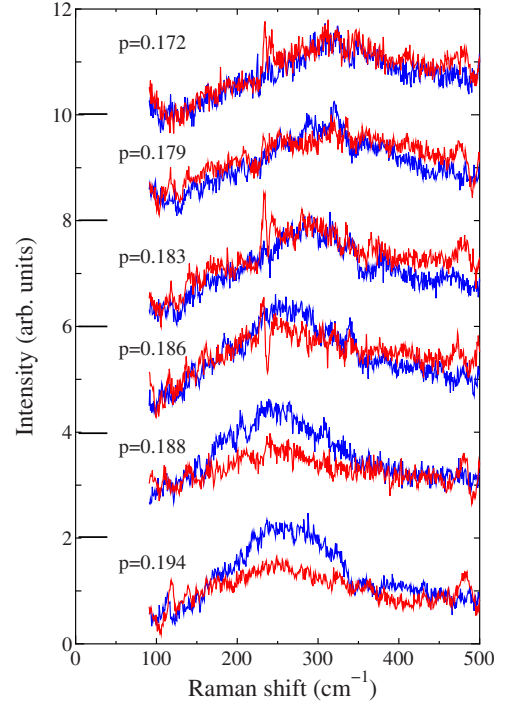


FIG. 4. (Color online) XX - and YY -polarized Raman-scattering spectra at 10 K for various doping levels. The dark (blue in color) and the light (red in color) curves represent the XX and YY spectra, respectively. Phonon peaks are subtracted by fitting.

direction,^{22,23} which results in a large anisotropy ratio γ of upper critical fields. As we reported in Ref. 24 γ rapidly decreases with overdoping and reaches the band calculation value (~ 3) at $p \sim 0.18$. This is another support for the recovering of three dimensionality observed in the YY spectrum and for the presence of critical doping at $p=0.19$ where the pseudogap closes.

For the anomalous doping dependence of A_{1g} and B_{1g} pair-breaking peaks, we need more careful discussion. Four possible factors can be listed up as origins for the decrease in the pair-breaking peak energies: (i) decrease in the maximum gap energy Δ_0 with doping due to T_c suppression, (ii) mixing of the s -wave component with doping, (iii) change in the topology of Fermi surface (FS) with doping, and (iv) change in the Fermi surface around $(0, \pm\pi)$ and $(\pm\pi, 0)$ by collapse of the pseudogap. It is clear that the first one is not the sole origin to explain the observed rapid decrease in pair-breaking peaks. Some or all of the other three may contribute to this phenomenon. The second origin, the s -wave mixing, is currently the most plausible explanation to reconcile with the observed rapid change in Raman spectra, although the origin of the s -wave component is unclear yet. As the s -wave component increases with doping, the energy of B_{1g} pair breaking radically decreases because of the appearance of the smaller gap maximum as well as the screening effect in the B_{1g} channel.²⁰ The screening effect also suppresses the A_{1g} peak intensity.

The third one, the FS topology, should also be taken into account because the \mathbf{k} dependence of superconducting gap energy depends on the shape of FS even for the case of simple d -wave gap. Moreover, the B_{1g} Raman vertex is quite

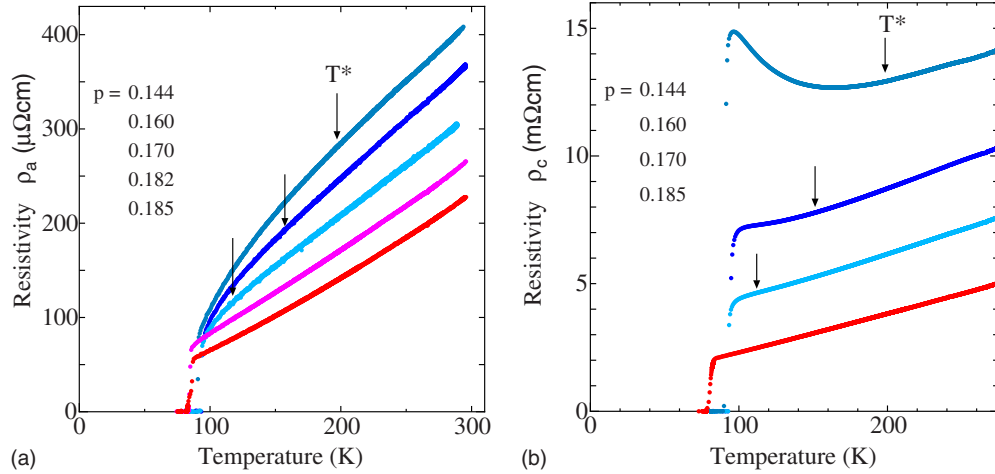


FIG. 5. (Color online) Resistivities of Y/Ca-123. (a) In-plane resistivities ρ_a . Arrows indicate T^* where temperature dependence deviates from T -linear dependence. (b) c -axis resistivities ρ_c . Arrows indicate T^* where low-temperature upturn of resistivities starts.

sensitive to the FS topology in the antinodal direction where Van Hove singularity is present. According to the calculation by Branch and Carbotte,²⁵ the B_{1g} peak energy changes with the second-nearest hopping t' because the FS topology changes with t' from holelike to an electronlike one. The change from holelike FS to an electronlike one was reported by ARPES for $\text{La}_{2-x}\text{Sr}_x\text{CuO}_4$ with $x \sim 0.22$.²⁶ Although so far there is no information about the FS topology of overdoped YBCO, a similar FS change, if it exists, can be a part of the sources for the observed anomalies in Raman spectra. However, the estimated reduction in the B_{1g} peak energy is 30% at most by the change in FS topology.

Since the B_{1g} Raman spectrum is sensitive to the FS around $(\pm\pi, 0)$ and $(0, \pm\pi)$, disappearance of the pseudogap (the fourth factor) must seriously affect the B_{1g} spectrum. The next question is which of these four factors can cause the nonmonotonic change in the A_{1g} and B_{1g} pair-breaking peaks. The first factor (decrease in Δ_0) can be ruled out because it is unlikely that Δ_0 abruptly changes at $p = 0.19$. The observed spectral change at $p \sim 0.19$ should be rather attributed to the FS change in the antinodal direction, in particular, to the closing of the pseudogap.

Similar anomalous changes in Raman spectra at a certain critical doping were also observed for $\text{Tl}_2\text{Ba}_2\text{CuO}_z$,^{27–29} and thus this should be common among HTSCs. Although one may expect that the collapse of pseudogap in overdoped regime leads to a simple d -wave superconductivity, the observed anomaly in this study is quite distinct from such a simple superconducting state. Here we may take into consideration the existence of unpaired carriers in the overdoped regime. For example, a large amount of unpaired carriers are observed in far-infrared spectra,³⁰ specific heat,³¹ and magnetic susceptibility.³² If a superconducting phase and un-

paired carriers coexist, a proximity effect between the two phases must be taken into account. This could induce an anomaly such as an s -wave component. An abrupt change at $p = 0.19$ suggests that this proximity effect may change where the FS is fully recovered.

V. SUMMARY

In order to examine the phase diagram from the viewpoint of superconducting response, we studied the electronic Raman spectra of overdoped $(\text{Y, Ca})\text{Ba}_2\text{Cu}_3\text{O}_y$ as a function of doping level p . By a precise and systematic study on a series of detwinned crystals with various Ca and oxygen contents, we were able to remove the contribution of oxygen deficiency in our discussion and to extract a pure doping effect.

It was found that the changes in superconducting responses in XX/YY and A_{1g}/B_{1g} polarizations are not monotonic but show abrupt changes at around $p = 0.19$, where the closing of the pseudogap is suggested by both $\rho_a(T)$ and $\rho_c(T)$. These changes at $p = 0.19$ are attributed to an essential change in the electronic state such as the closing of the pseudogap and the change in Fermi-surface topology. Our results support the picture in which the pseudogap line $T^*(p)$ hits zero at $p \sim 0.19$ in the phase diagram for Y123. The negative quantum interference in Raman scattering and the anisotropy ratio of upper critical fields suggest a three-dimensional electronic state above $p = 0.19$, while the normal-state resistivity indicates a persistence of unusual charge dynamics along the c axis.

ACKNOWLEDGMENT

This work was supported by the New Energy and Industrial Technology Development Organization (NEDO) as Collaborate Research and Development of Fundamental Technologies for Superconductivity Applications.

*tmasui@phys.sci.osaka-u.ac.jp

- ¹J. B. Torrance, Y. Tokura, A. I. Nazzal, A. Bezinge, T. C. Huang, and S. S. P. Parkin, *Phys. Rev. Lett.* **61**, 1127 (1988).
- ²T. Timusk and B. Statt, *Rep. Prog. Phys.* **62**, 61 (1999).
- ³J. L. Tallon and J. W. Loram, *Physica C* **349**, 53 (2001).
- ⁴S. Pailhes, C. Ulrich, B. Fauque, V. Hinkov, Y. Sidis, A. Ivanov, C. T. Lin, B. Keimer, and P. Bourges, *Phys. Rev. Lett.* **96**, 257001 (2006).
- ⁵D. van der Marel, H. J. A. Molegraaf, J. Zaanen, Z. Nussinov, F. Carbone, A. Damascelli, H. Eisaki, M. Greven, P. H. Kes, and M. Li, *Nature (London)* **425**, 271 (2003).
- ⁶N. Gedik, M. Langner, J. Orenstein, S. Ono, Y. Abe, and Y. Ando, *Phys. Rev. Lett.* **95**, 117005 (2005).
- ⁷G. S. Boebinger, Y. Ando, A. Passner, T. Kimura, M. Okuya, J. Shimoyama, K. Kishio, K. Tamasaku, N. Ichikawa, and S. Uchida, *Phys. Rev. Lett.* **77**, 5417 (1996).
- ⁸N. Nagaosa and P. A. Lee, *Phys. Rev. Lett.* **64**, 2450 (1990).
- ⁹T. Tanamoto, H. Kohno, and H. Fukuyama, *J. Phys. Soc. Jpn.* **63**, 2739 (1994).
- ¹⁰V. J. Emery and S. A. Kivelson, *Nature (London)* **374**, 434 (1995).
- ¹¹T. Stauffer, R. Nemschek, R. Hackl, P. Müller, and H. Veith, *Phys. Rev. Lett.* **68**, 1069 (1992).
- ¹²T. Masui, M. Limonov, H. Uchiyama, S. Lee, S. Tajima, and A. Yamanaka, *Phys. Rev. B* **68**, 060506(R) (2003).
- ¹³T. Masui, M. Limonov, H. Uchiyama, S. Tajima, and A. Yamanaka, *Phys. Rev. Lett.* **95**, 207001 (2005).
- ¹⁴Y. Yamada and Y. Shiohara, *Physica C* **217**, 182 (1993).
- ¹⁵B. Fisher, J. Genossar, C. G. Kuper, L. Patlagan, G. M. Reisner, and A. Knizhnik, *Phys. Rev. B* **47**, 6054 (1993).
- ¹⁶J. L. Tallon, C. Bernhard, H. Shaked, R. L. Hitterman, and J. D. Jorgensen, *Phys. Rev. B* **51**, 12911 (1995).
- ¹⁷M. Limonov, D. Shantsev, S. Tajima, and A. Yamanaka, *Phys. Rev. B* **65**, 024515 (2001).
- ¹⁸X. K. Chen, E. Altendorf, J. C. Irwin, R. Liang, and W. N. Hardy, *Phys. Rev. B* **48**, 10530 (1993).
- ¹⁹T. P. Devereaux and D. Einzel, *Phys. Rev. B* **51**, 16336 (1995).
- ²⁰R. Nemschek, R. Hackl, M. Opel, R. Philipp, M. T. Béal-Monod, J. B. Bieri, K. Maki, A. Erb, and E. Walker, *Eur. Phys. J. B* **5**, 495 (1998).
- ²¹K. Takenaka, K. Mizuhashi, H. Takagi, and S. Uchida, *Phys. Rev. B* **50**, 6534(R) (1994).
- ²²K. Semba, A. Matsuda, and T. Ishii, *Phys. Rev. B* **49**, 10043 (1994).
- ²³K. Tomimoto, I. Terasaki, A. I. Rykov, T. Mimura, and S. Tajima, *Phys. Rev. B* **60**, 114 (1999).
- ²⁴K. Nagasao, T. Masui, and S. Tajima, *Physica C* **468**, 1188 (2008).
- ²⁵D. Branch and J. P. Carbotte, *Phys. Rev. B* **54**, 13288 (1996).
- ²⁶A. Ino, C. Kim, M. Nakamura, T. Yoshida, T. Mizokawa, A. Fujimori, Z.-X. Shen, T. Kakeshita, H. Eisaki, and S. Uchida, *Phys. Rev. B* **65**, 094504 (2002).
- ²⁷C. Kendziora, R. J. Kelley, and M. Onellion, *Phys. Rev. Lett.* **77**, 727 (1996).
- ²⁸L. V. Gasparov, P. Lemmens, N. N. Kolesnikov, and G. Güntherodt, *Phys. Rev. B* **58**, 11753 (1998).
- ²⁹T. Nishikawa, T. Masui, S. Tajima, H. Eisaki, H. Kito, and A. Iyo, *J. Phys. Chem. Solids* **69**, 3074 (2008).
- ³⁰J. Schützmann, S. Tajima, S. Miyamoto, and S. Tanaka, *Phys. Rev. Lett.* **73**, 174 (1994); J. Schützmann, S. Tajima, S. Miyamoto, Y. Sato, and I. Terasaki, *Solid State Commun.* **94**, 293 (1995).
- ³¹J. W. Loram, J. L. Tallon, and W. Y. Liang, *Phys. Rev. B* **69**, 060502(R) (2004).
- ³²Y. Tanabe, T. Adachi, T. Noji, and Y. Koike, *J. Phys. Soc. Jpn.* **74**, 2893 (2005).